

# Journal Pre-proof

Spatial resolution of drug crystallisation in the skin by X-ray micro-computed tomography

Choon Fu Goh, Daniel O'Flynn, Robert Speller, Majella E. Lane



PII: S0968-4328(21)00036-6  
DOI: <https://doi.org/10.1016/j.micron.2021.103045>  
Reference: JMIC 103045

To appear in: *Micron*

Received Date: 11 December 2020  
Revised Date: 3 February 2021  
Accepted Date: 27 February 2021

Please cite this article as: Goh CF, O'Flynn D, Speller R, Lane ME, Spatial resolution of drug crystallisation in the skin by X-ray micro-computed tomography, *Micron* (2021), doi: <https://doi.org/10.1016/j.micron.2021.103045>

This is a PDF file of an article that has undergone enhancements after acceptance, such as the addition of a cover page and metadata, and formatting for readability, but it is not yet the definitive version of record. This version will undergo additional copyediting, typesetting and review before it is published in its final form, but we are providing this version to give early visibility of the article. Please note that, during the production process, errors may be discovered which could affect the content, and all legal disclaimers that apply to the journal pertain.

© 2020 Published by Elsevier.

Spatial resolution of drug crystallisation in the skin by X-ray micro-computed tomography

Choon Fu Goh <sup>a, b, \*</sup>, Daniel O'Flynn <sup>c</sup>, Robert Speller <sup>c</sup>, Majella E. Lane <sup>b</sup>

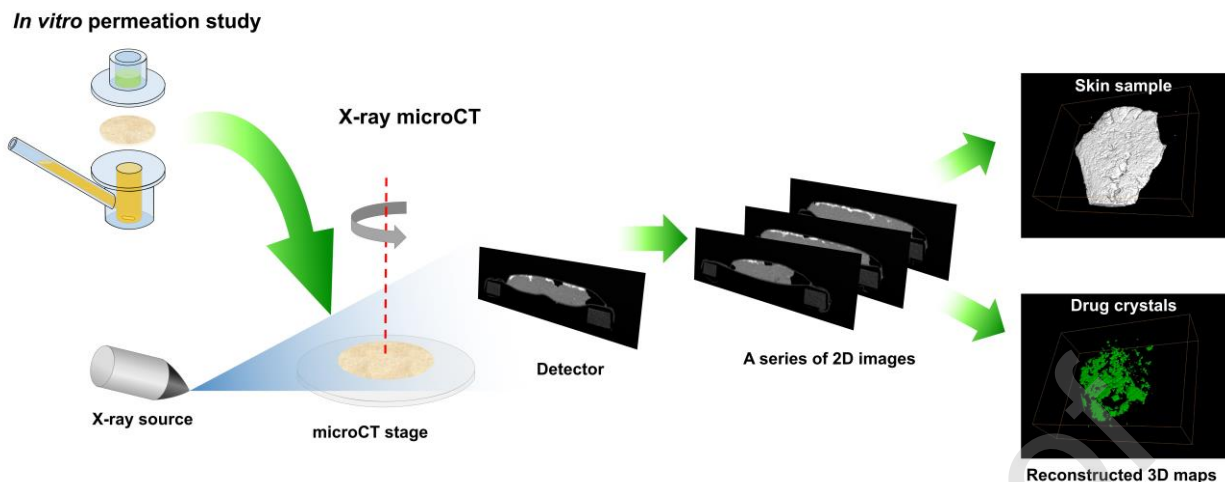
<sup>a</sup> Discipline of Pharmaceutical Technology, School of Pharmaceutical Sciences, Universiti Sains Malaysia, 11800 Minden, Penang, Malaysia

<sup>b</sup> Department of Pharmaceutics, UCL School of Pharmacy, 29-39 Brunswick Square, London WC1N 1AX, United Kingdom

<sup>c</sup> Department of Medical Physics and Biomedical Engineering, University College London, Gower Street, London WC1E 6BT, United Kingdom

\* Corresponding author: Choon Fu Goh. Discipline of Pharmaceutical Technology, School of Pharmaceutical Sciences, Universiti Sains Malaysia, 11800 Minden, Penang, Malaysia.  
Tel: +604-6532074. Fax: +604-6570017. Email: choonfugoh@usm.my

**Graphical abstract**



### Highlights:

- First report of microCT to study drug crystallisation phenomenon in the skin
- Evidences of isolated drug crystal clusters embedded up to 0.2 – 0.3 mm in the skin
- Lateral junctions between corneocytes and hair follicles are potential “hotspots”
- A non-destructive way to profile drug crystal distribution in deeper skin layers

### ABSTRACT:

Drug crystallisation in the skin is recognised as a significant problem in topical and transdermal drug delivery. Our recent investigations provided new evidence of drug crystallisation in the skin, however, confirming the precise location of crystals remains challenging. Of note, most approaches used have required disruption of the membrane by tape stripping, with crystal detection limited to the superficial skin layers. Hence, a non-destructive method for complete spatial resolution of crystallised drug in skin is still lacking. In this communication, we report the application of X-ray micro-computed tomography (microCT) to examine drug crystallisation in mammalian skin *ex vivo*. Permeation studies of a saturated solution of diclofenac sodium were conducted in

porcine skin; subsequently, tissue samples were scanned using microCT to generate 2D and 3D maps. A layer of drug crystals was observed on the skin surface; microCT maps also confirmed the distribution of drug crystals up to a skin depth of 0.2 – 0.3 mm. MicroCT also allowed the identification of drug crystallisation as a distinct and confirmed event in the skin and as an extension from drug crystals formed on the skin. These preliminary results confirm the potential of microCT to study this important phenomenon in topical and transdermal drug delivery.

**ABBREVIATIONS:**

DF Na: Diclofenac sodium

MicroCT: micro-computed tomography

PG: Propylene glycol

**KEYWORDS:**

microCT; drug crystallisation; porcine ear skin; diclofenac sodium; topical and transdermal drug delivery

**MANUSCRIPT BODY:**

The problem of drug crystallisation in the skin, following topical application of formulations, remained a hypothesis until relatively recently. However, recent

investigations from our group have now confirmed this phenomenon, both *in vitro* (Goh et al., 2017a; Goh et al., 2019; Goh et al., 2020) and *in vivo* (Hadgraft and Lane, 2016). These studies employed various characterisation techniques, including spectroscopic and localised nano-thermal and synchrotron SAXS/WAXS analyses; drug crystals were identified in the skin following topical application of various formulations to mammalian skin. As well as requiring tape stripping, the major limitation in the ATR-FTIR study that we reported was the inability to detect crystals in the deeper layers of the skin (Goh et al., 2017a). This is not surprising because the weak IR signals from the drug crystals were totally masked by a stronger IR spectrum from the skin samples in the stripped tapes. The difficulty in identifying the overlapped IR signals of drug crystals is the main hurdle for this characterisation method. In a later investigation we reported the use of thermal and spectroscopic probe-based microscopies to study crystallised drug in skin. However this approach is time consuming even for complete scanning of a small area of tissue, that must also be collected on tape strips (Goh et al., 2019). Again with this approach it is difficult to locate the drug crystals of smaller size in the deeper skin layers. Finally, even though sequential step-scans from the skin surface to the inner skin layers were collected using SAXS/WAXS analysis, multiple horizontal scans across the skin sample have to be performed repetitively to locate drug crystal diffractions (Goh et al., 2020).

X-ray micro-computed tomography (microCT) is typically used to inspect internal features of solid objects with high resolution. The non-destructive nature of microCT allows three-dimensional (3D) visualisation and analysis of samples at both the macro- and micro-scales. Unlike conventional X-ray diffraction techniques, microCT allows the absorption of X-rays by objects to varying degrees instead of reflections to create a series

of two-dimensional (2D) X-ray images. The contrast in microCT images is generated as a result of the differences in electron density unique to various elements. Reconstruction of a 3D image can be achieved by combining a series of 2D projections. To date, this technique has not been used extensively in drug delivery research. Previously, microCT was demonstrated to be an advanced solid state characterisation technique that provides insights into phase separation of drugs via visualisation of drug crystal distribution in solid dispersions (Alhijaj et al., 2015; Alhijaj et al., 2017). Given that skin samples and drug crystals are two fundamentally different materials, we hypothesised that microCT should be capable of resolving this complex composite effectively. The selectivity of microCT in for analysis of solid objects only is advantageous in the present study and more importantly, microCT is a non-destructive technique that requires no sample preparation such as tape stripping. In addition, microCT can provide a comprehensive overview of the whole internal structure of an object without requiring manual and repetitive scanning of different parts of a sample. The motivation of this study was, therefore, to investigate the spatial resolution of drug crystallisation in the skin using microCT, following application of a saturated drug solution to mammalian skin.

In this work, we carried out an *in vitro* permeation study using Franz-type diffusion cells (diffusional area =  $\sim 1 \text{ cm}^2$ ) as detailed previously (Goh et al., 2017b, 2019). Fresh porcine ears sourced from a local abattoir were washed with deionised water before isolating the outer skin membrane. The prepared tissue was stored at  $-20^\circ\text{C}$  and thawed at room temperature before use. The skin was sandwiched between the donor and receptor chambers of Franz-type diffusion cells with the outer skin membrane facing upward. The receptor chamber was filled with phosphate buffered saline ( $\text{pH } 7.3 \pm 0.2$ ).

Once the skin membrane temperature had equilibrated to  $32 \pm 0.5^\circ\text{C}$ , the donor chamber was loaded with  $10 \mu\text{L}/\text{cm}^2$  of a saturated solution of diclofenac sodium (DF Na) in propylene glycol (PG) for 24 h. DFNa is a topical nonsteroidal anti-inflammatory drug that is commonly used to relieve pain and inflammation (Goh and Lane, 2014). PG was selected to ensure high loading and thermodynamic activity of the drug substance in the solvent as reported earlier (Goh et al., 2020). PG has previously been reported to penetrate and be cleared from the skin barrier more rapidly than a number of drugs (Trottet et al., 2004). This solvent loss from the formulation is expected to create a high thermodynamic state of drugs *in situ* in the skin, leading to supersaturation and ultimately drug crystallisation. After 24 h, the Franz-type diffusion cells were disassembled and the skin membrane was carefully removed. The skin sample was wrapped with Parafilm™ to avoid tissue dehydration and mounted onto a plastic holder for the microCT scan. The microCT scan was repeated with a control skin sample.

A benchtop cone-beam microCT system (Nikon Metrology, X-Tek, UK) equipped with a microfocus X-ray tube ( $12 \mu\text{m}$  focal spot, 50 kV) was used for all experiments. The source to detector distance was fixed at 688 mm. The number of projections was 1026 with an average of 64 frames for each projection. CT image reconstruction was carried out using the in-built X-Tek software (Nikon Metrology, X-Tek, UK). The analysis of the images was performed using MicroView Version 2.6.0-3 (GE Healthcare Biosciences) to visualise the skin samples as 2D and 3D maps (resolution:  $23 \mu\text{m}$ ) for different areas of the skin and drug crystals.

Fig. 1 and Fig. 2 show selected 2D maps of the skin sample slicing at the x and z axis after the 24 h permeation study. There are three distinctive colour domains observed

in the maps – white, light grey and dark grey. The grey zones represent the skin sample while the dark grey zone corresponds to the sample holder and Parafilm™ which was confirmed by analysis of a control skin sample (data not shown). The white areas located at the top of the skin sample are the drug crystals. The colour contrast arises from the difference in the absorption of X-rays by the materials as a result of the variations of density and atomic number. As shown in these images some white areas are surrounded by light grey domains. This is consistent with drug penetration into the skin followed by drug precipitation as separate crystal clusters in the skin. The vertical section view of the skin sample is shown in Fig. 3 where drug crystals were found to extend into the skin layers. In particular, drug crystal growth occurred along the lateral junctions between the penta- or hexagonal-shaped corneocytes and the appendages such as hair follicles. It might be speculated that these regions enriched with drug crystals may be “hotspots” to trigger further drug crystallisation in the inner skin layers.



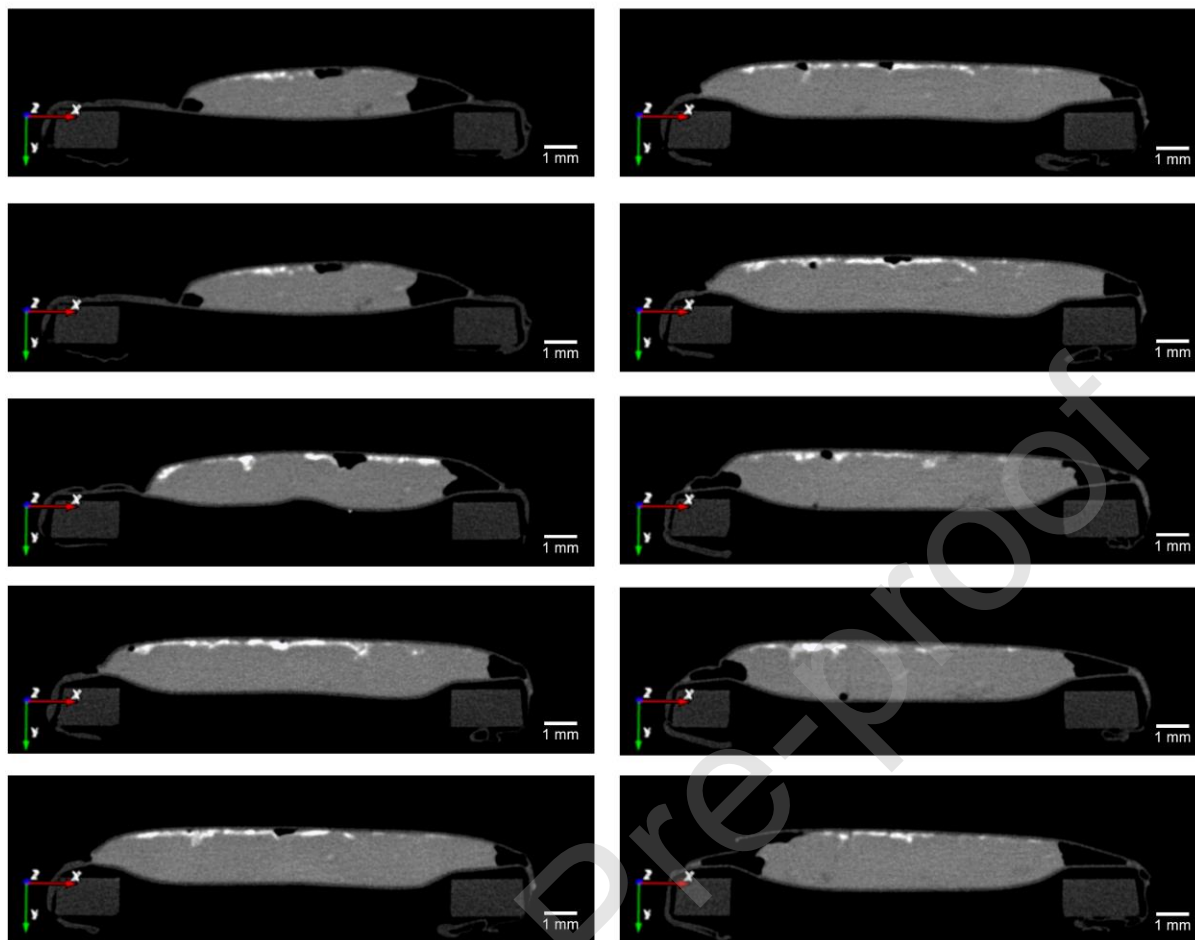
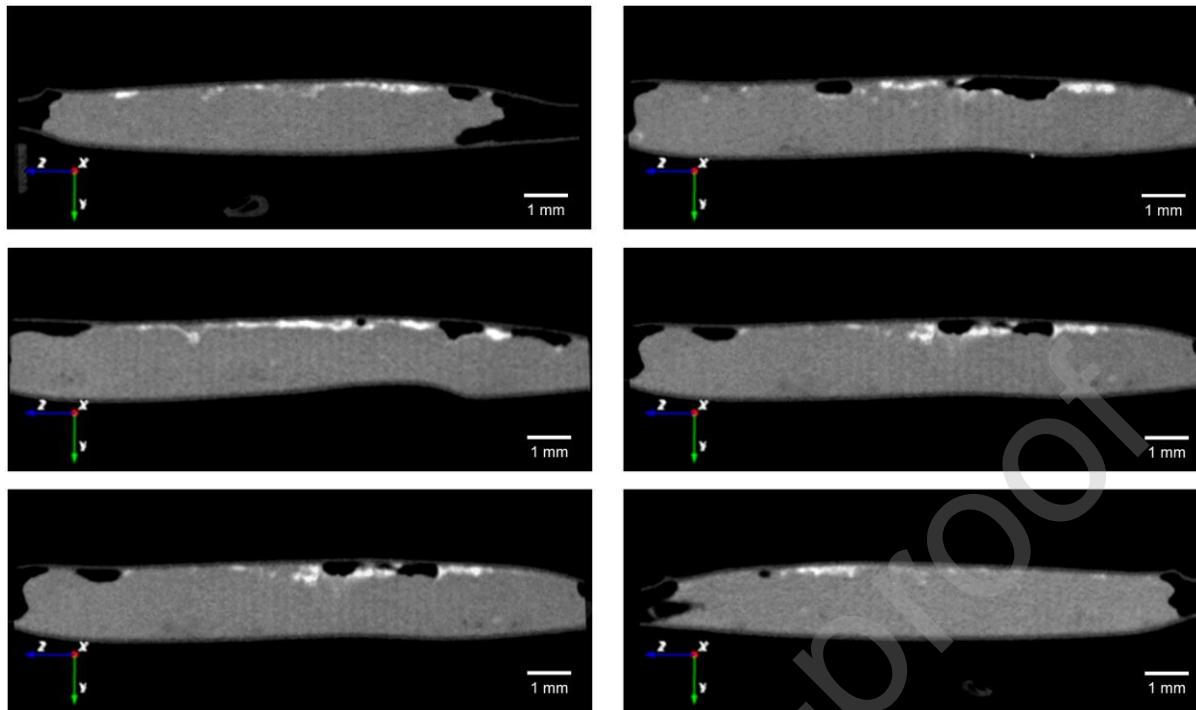
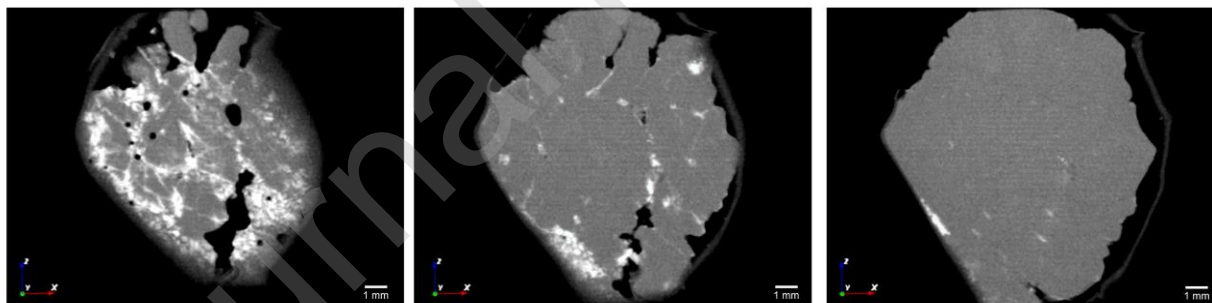


Fig. 1 2D microCT images of skin sample slicing at the z axis after 24 h permeation study



**Fig. 2** 2D microCT images of skin sample slicing at the x axis after 24 h permeation study



**Fig. 3** 2D microCT images of skin sample slicing at y axis after 24 h permeation study (left to right: top to inner skin layers)

For better visualisation, the 2D slice-by-slice information were combined to form reconstructed 3D maps in order to determine crystal distribution in the skin. This provides confidence that actual crystals in the skin are profiled rather than any protruding drug crystals from the skin surface. Movie 1 shows the 3D rotation of (A) the skin sample after the permeation experiment and (B) the isolated drug crystals from this sample. There are several individual drug crystal clusters (highlighted with the red circle) that are isolated from the drug crystal layer on the skin as shown in Fig. 4 (Movie 2) and Fig. 5 (Movie 3). The images in Fig. 4C – D and Fig. 5C – D are vertically flipped to show the drug crystal clusters embedded in the inner skin layers. These observations confirm the formation of isolated drug crystals in the skin rather than extensions of crystal growth from the skin surface.

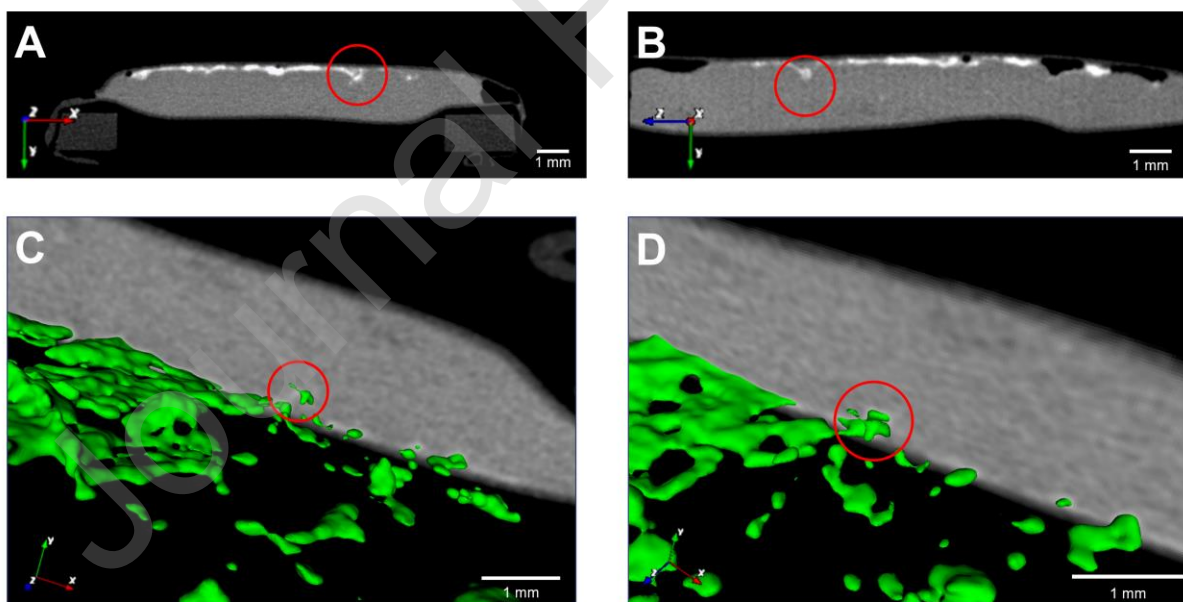


**Fig. 4** 2D microCT images of skin sample slicing at (A) x and (B) z axes and (C – D) 3D maps (vertically flipped) showing drug crystals (green colour) in different projections after 24 h permeation study. The isolated drug crystal cluster is highlighted in the red circles.

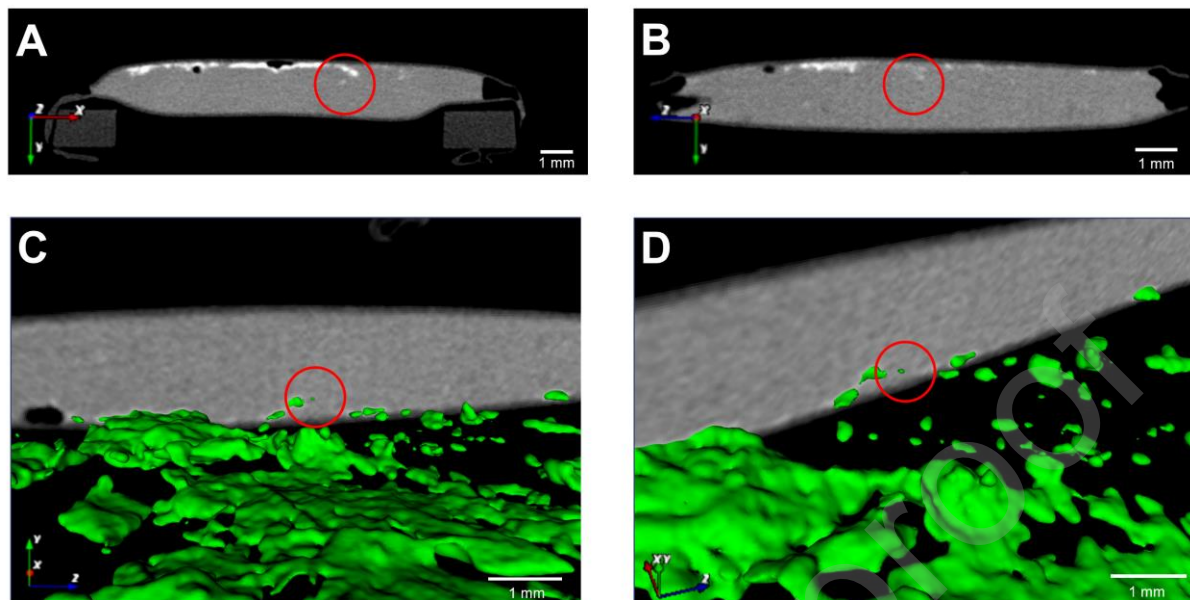


**Fig. 5** 2D microCT images of skin sample slicing at (A) x and (B) z axes and (C – D) 3D maps (vertically flipped) showing drug crystals (green colour) in different projections after 24 h permeation study. The isolated drug crystal cluster is highlighted in the red circles.

Drug distribution in the skin was evaluated using confocal Raman spectroscopy (CRS) in an *ex vivo* permeation study applying the same DF Na formulation in PG on the porcine ear skin for 30 min as described previously (Goh et al., 2020). Because of the high drug thermodynamic activity of the saturated drug solution, the permeation was conducted in a shorter time period to allow precise observation of drug distribution without affecting drug crystals during CRS analysis. Although the drug intensity is expressed in arbitrary units (a.u.) because of the semi-quantitative nature of the analysis, DF Na was reported to penetrate up to  $\sim 20\ \mu\text{m}$  in porcine skin as shown in Fig. 6. The observation of drug crystal diffractions in WAXS profiles was evident up to  $10\ \mu\text{m}$  in the skin which corresponds to the reported thickness of porcine stratum corneum (Klang et al., 2011;

Mahrhauser et al., 2015). In the current study, it is interesting to note that drug crystals appeared as isolated clusters embedded in the skin structure at a depth of up to 0.2 – 0.3 mm. Previous work with SAXS/WAXS analysis only recorded the formation of drug crystals up to 20 – 25  $\mu\text{m}$  (Goh et al., 2020). The spatial resolution capability of microCT therefore allows the detection of drug crystals *in situ* in deeper skin layers. This imaging technique also enables the differentiation of isolated drug crystal clusters in the skin from the bulk drug crystal layer on the skin. To our knowledge this has not been reported to date. Considering that microCT only allows a spatial resolution within the micrometre range (23  $\mu\text{m}$  in this work), any drug crystals with sizes smaller than a few microns would not be resolved.

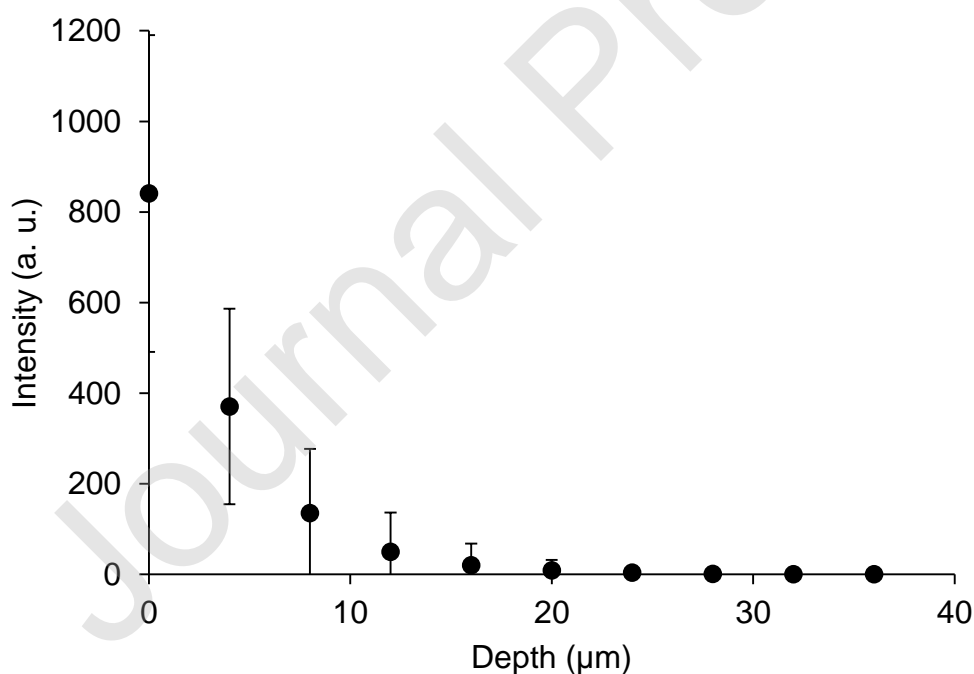


**Fig. 6 CRS depth profiles of drug for the *ex vivo* permeation experiment with a saturated solution of DFNa in PG**

Despite recent advances in our understanding of drug crystallisation or “metamorphosis” in the epidermis, spatial resolution of crystals in organic tissues of very fine structure such as the skin remains challenging. This communication is the first report of the use of microCT to detail the composite structure of skin samples with entrapped drug crystals. Capturing drug crystals in the skin is challenging due to the unpredictable nature of drug crystallisation. The non-destructive method reported here profiles the spatial distribution of drug crystal clusters on and in the skin with an ability to locate their exact positions. More importantly, we now have an understanding of the fundamental characteristics of drug crystal growth and accumulation at the boundary between corneocytes and in the hair follicles before reaching the inner skin layers. This preliminary work with microCT analysis warrants further investigations using related characterisation tools with a higher resolution, such as nanoCT, to advance our current understanding of drug crystallisation in biological membranes and the related mechanisms. In the longer term the ability to study and predict this problem will allow for a more rational formulation design approach in topical and transdermal delivery.

**Author contributions:**

Choon Fu Goh and Daniel O’Flynn designed the research, performed the experiments and data analysis. Choon Fu Goh drafted the manuscript. Robert Speller and Majella E. Lane revised the manuscript. All of the authors have read and approved the final manuscript

**Declaration of competing interest:**

The authors have no conflicts of interest to declare.

**REFERENCES:**

Alhijaj, M., Bouman, J., Wellner, N., Belton, P., Qi, S., 2015. Creating drug solubilization compartments via phase separation in multicomponent buccal patches prepared by direct hot melt extrusion–injection molding. *Mol Pharm* 12, 4349-4362.

Alhijaj, M., Yassin, S., Reading, M., Zeitler, J.A., Belton, P., Qi, S., 2017. Characterization of Heterogeneity and Spatial Distribution of Phases in Complex Solid Dispersions by Thermal Analysis by Structural Characterization and X-ray Micro Computed Tomography. *Pharm Res* 34, 971-989.

Goh, C.F., Boyd, B.J., Craig, D.Q.M., Lane, M.E., 2020. Profiling of drug crystallization in the skin. *Expert Opin Drug Deliv* 17, 1321-1334.

Goh, C.F., Craig, D.Q.M., Hadgraft, J., Lane, M.E., 2017a. The application of ATR-FTIR spectroscopy and multivariate data analysis to study drug crystallisation in the stratum corneum. *Eur J Pharm Biopharm* 111, 16-25.

Goh, C.F., Lane, M.E., 2014. Formulation of diclofenac for dermal delivery. *Int J Pharm* 473, 607-616.

Goh, C.F., Moffat, J.G., Craig, D.Q.M., Hadgraft, J., Lane, M.E., 2017b. Nano-thermal imaging of the stratum corneum and its potential use for understanding of the mechanism of skin penetration enhancer. *Thermochim Acta* 655, 278-283.

Goh, C.F., Moffat, J.G., Craig, D.Q.M., Hadgraft, J., Lane, M.E., 2019. Monitoring Drug Crystallization in Percutaneous Penetration Using Localized Nanothermal Analysis and Photothermal Microspectroscopy. *Mol Pharm* 16, 359-370.

Hadgraft, J., Lane, M.E., 2016. Drug crystallization – implications for topical and transdermal delivery. *Expert Opin Drug Deliv* 13, 817-830.

Klang, V., Schwarz, J.C., Hartl, A., Valenta, C., 2011. Facilitating *in vitro* tape stripping: Application of infrared densitometry for quantification of porcine stratum corneum proteins. *Skin Pharmacol Physiol* 24, 256-268.

Mahrhauser, D.-S., Nagelreiter, C., Gehrig, S., Geyer, A., Ogris, M., Kwizda, K., Valenta, C., 2015. Assessment of Raman spectroscopy as a fast and non-invasive method for total stratum corneum thickness determination of pig skin. *Int J Pharm* 495, 482-484.

Trottet, L., Merly, C., Mirza, M., Hadgraft, J., Davis, A.F., 2004. Effect of finite doses of propylene glycol on enhancement of *in vitro* percutaneous permeation of loperamide hydrochloride. *Int J Pharm* 274, 213-219.



1 **FIGURE LEGENDS:**

2 Fig. 1 2D microCT images of skin sample slicing at the z axis after 24 h permeation study

3 Fig. 2 2D microCT images of skin sample slicing at the x axis after 24 h permeation study

4 Fig. 3 2D microCT images of skin sample slicing at y axis after 24 h permeation study

5 (left to right: top to inner skin layers)

6 Fig. 4 2D microCT images of skin sample slicing at (A) x and (B) z axes and (C – D) 3D

7 maps (vertically flipped) showing drug crystals (green colour) in different projections after

8 24 h permeation study. The isolated drug crystal cluster is highlighted in the red circles.

9 Fig. 5 2D microCT images of skin sample slicing at (A) x and (B) z axes and (C – D) 3D

10 maps (vertically flipped) showing drug crystals (green colour) in different projections after

11 24 h permeation study. The isolated drug crystal cluster is highlighted in the red circles.

12 Fig. 6 CRS depth profiles of drug for the ex vivo permeation experiment with a saturated

13 solution of DFNa in PG

14

15 **MOVIE LEGENDS:**

16 Movie 1 3D rotation showing (A) the skin sample after 24 h permeation study and (B) the

17 corresponded drug crystals

18 Movie 2 3D slicing at y axis (vertically flipped) showing the isolated drug crystals illustrated

19 in Figure 4. The isolated drug crystal cluster is highlighted in the red circle.

20 Movie 3 3D slicing at x axis (vertically flipped) showing the isolated drug crystals illustrated

21 in Figure 5. The isolated drug crystal cluster is highlighted in the red circle.